ADVANCED FUNCTIONAL MATERIALS
www.afm-journal.de

Enhancing Light Emission of Nanostructured Vertical Light-Emitting Diodes by Minimizing Total Internal Reflection

Byeong-Uk Ye, Buem Joon Kim, Yang Hee Song, Jun Ho Son, Hak ki Yu, Myung Hwa Kim, Jong-Lam Lee, and Jeong Min Baik**

Nanostructured vertical light-emitting diodes (V-LEDs) with a very dense forest of vertically aligned ZnO nanowires on the surface of N-face n-type GaN are reported with a dramatic improvement in light extraction efficiency (~3.0×). The structural transformation (i.e., dissociation of the surface nitrogen atoms) at the nanolevel by the UV radiation and Ozone treatments contributes significantly to the initial nucleation for the nanowires growth due to the interdiffusion of Zn into GaN, evident by the scanning photoemission microscopy (SPEM), high-resolution transmission electron microscopy (HR-TEM), and ultraviolet photoelectron spectroscopy (UPS) measurements. This enables the growth of densely aligned ZnO nanowires on N-face n-type GaN. This approach shows an extreme enhancement in light extraction efficiency (>2.8×) compared to flat V-LEDs, in good agreement with the simulation expectations (~3.01×) obtained from 3D finite-difference time-domain (FDTD) tools, explained by the wave-guiding effect. The further increase (~30%) in light extraction efficiency is also observed by optimized design of nanogeometry (i.e., MgO layer on ZnO nanorods).

1. Introduction

GaN-based light-emitting diodes (LEDs) have revolutionized solid-state lighting and large displays, due to their reliably long life, short response time, high radiance, and low energy consumption.[1,2] N-side-up InGaN verticalLEDs (V-LEDs) fabricated by laser lift-off (LLO) have been suggested to be the most promising candidates as high-power LEDs.[3,4] Although the internal quantum efficiency (IQE) for blue LEDs is as high as 70%,[5] the external quantum efficiency (EQE) is still low due to the low light extraction efficiency because most of the photons generated in the active region still remain inside the LEDs owing to the total internal reflection (TIR) at the interface of the semiconductor with air.[6] To date, several methods have been proposed to improve the light extraction efficiency,[7–11] however, an additional passivation process is required[12] or conventional photolithography is not available, limiting the usefulness of these methods.

Recently, the use of one-dimensional (1D) ZnO nanostructures synthesized by hydrothermal synthesis to fabricate nanostructured hybrid LEDs is expected to be an attractive alternative by utilizing its excellent optical and electrical properties, high transparency, and lower refractive index (~2.0) than that of GaN (~2.5).[13–17] However, the reported data so far show low extraction efficiency (~0%), possibly as a result of TIR between the seed layer and GaN since ZnO seed layers are required for growing the highly-dense ZnO nanowires.

Here, we report an extreme increase in the light extraction efficiency (~3.0×) of GaN-based V-LEDs, assisted by the epitaxial growth of ZnO nanorods on N-face n-type GaN without any seeds by the modification of the structures (at the nanolevel) on the surface. Wurtzite GaN is a polar material that has two different planes along its *c*-axis. The (0001) plane is the Ga-terminated face while the $(000\bar{1})$ plane is the N-face (see the Figure 1S in the Supporting Information). It is well-known that the morphological, physical and chemical properties as well as the growth of the ZnO nanostructures depend greatly on the polarity.[18–20] To date, most research has been focused on the growth behavior of ZnO nanowires with the polarity, showing a strong preference for ZnO nanowires growth on Ga-face GaN. Here, such preference for growth of ZnO nanorods on Ga-face n-GaN is also shown, concomitant with changes in surface polarity (**Figure 1**). However, we will show that the strong surface polarity dependence disappears by UV radiation and Ozone treatment, resulted in growing highly-dense vertically aligned ZnO nanowires (nanorods) epitaxially on N-face n-type GaN without any seeds.

B.-U. Ye, Prof. J. M. Baik
School of Mechanical and Advanced Materials Engineering
Ulsan National Institute of Science and Technology (UNIST)
Ulsan 689-798, Republic of Korea
E-mail: jbaik@unist.ac.kr
B. J. Kim, Y. H. Song, Dr. J. H. Son, Dr. H. K. Yu, Prof. J.-L. Lee
Department of Materials Science and Engineering
Division of Advanced Materials Science
Pohang University of Science and Technology (POSTECH)
Pohang, Gyeongbuk 790-784, Republic of Korea
Email: jllee@postech.ac.kr
Prof. M. W. Kim
Department of Chemistry & Nano Science
Ewha Womans University
Seoul, 120-750, Republic of Korea

DOI: 10.1002/adfm.201101987

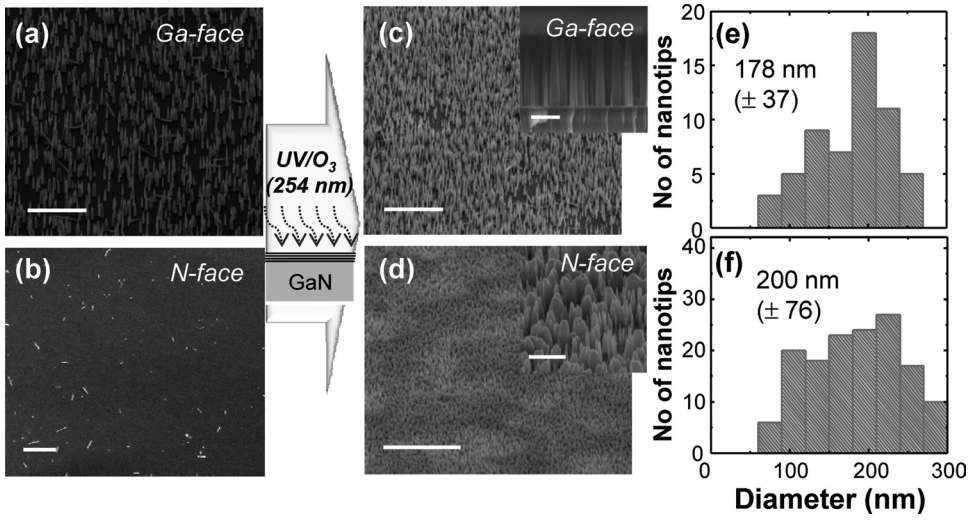

Figure 1. Scanning electron micrographs of ZnO nanorods grown on GaN substrates; a) as-grown Ga-face and b) as-grown N-face. Scanning electron microscopy (SEM) images of ZnO nanorods grown after ozone treatment assisted by UV radiation on c) Ga-face and d) N-face GaN substrates. The insets are the tilted view of ZnO nanorods (the scale bar is 500 nm). The nanorod growth was performed on a 2 inch sapphire wafer without any seed layer and the nanorods were formed over the whole wafer area. It is clearly found that the effect of surface polarity of the growth behavior disappeared after UV/Ozone treatment. A histogram of the size distribution of nanorods obtained at the middle point from the bottom for both samples (e,f). The scale bar is 10 μm.

2. Results and Discussion

2.1. Growth of Highly Dense ZnO Nanorods on N-Face n-Type GaN

Figure 1 shows the morphological evolution of ZnO nanorods grown on Ga-face and N-face GaN substrates with UV radiation and ozone treatment. The vertically well-aligned nanorods are already produced on the entire surface of Ga-face substrates (Figure 1a) and the density of the nanorods increased up to 4 times with the treatment (Figure 1c). A statistical analysis on the diameters (at the middle point) of 64 nanorods observed by the SEM image indicated that the majority clustered around an average diameter of 178 nm with a standard deviation of 37 nm, showing good uniformity (<20%) in diameter. The nanorod growth was performed on a 2 inch Ga-face GaN wafer without any seed layer and the nanorods were formed over the whole wafer area. On the other hand, there are no nanorods aligned vertically on the N-face surface and only a few things are distributed randomly, as shown in Figure 1b.

The preference for the growth on Ga-face GaN surfaces may be understood by the substrate-dependent kinetics of surface diffusion and desorption of the adatoms. For epitaxial layers of Ga-face GaN, the bound surface charge is negative through the spontaneous polarization, whereas for N-face GaN, the bound surface charge is positive. It is well-known that the electric charges present at the surface play crucial roles on growing the nanorods, due to the electrostatic interaction with ions (Zn^{2+} or OH^-) in the used precursors (zinc nitrate and HMT). The charged surface will attract ions of opposite charges (OH^- or Zn^{2+}) to it, creating a zinc oxide surface in turn.[21] However, this may not be strictly meaningful for the N-face GaN substrates, due to the few growth of nanorods. We must consider that the surface of N-face GaN is generally ended with nitrogen atoms, as reported previously.[22,23] Due to the relatively low binding energy between Zn and N, Zn-N bonds might not be stable and the Zn adatoms can easily desorb or diffuse along the surfaces for the N-face GaN substrates, increasing the diffusion length of the Zn adatoms. Thus, the growth of the ZnO nanorods on the N-face is not greatly favored and the more slow the growth rate of the ZnO nanorods.

Such a growth preference disappeared with UV radiation and ozone treatment. For the Ga-face GaN, the treatment increased the density of the nanorods up to 4 times (Figure 1c). Previously, we ascribed this to the formation of the heterogeneous surface structures at the nanolevel as well as the modification of surface stoichiometry.[24] For the N-face GaN, the density significantly increased by a factor of two more and most of them were grown with great vertical alignment (Figure 1d). Although the distribution in the diameter (± 76nm) is broader than that (± 37nm) of the nanorods grown on Ga-face substrates, due to the poor uniformity of the surface as N-face substrates are produced by exposing the GaN substrates in a laser lift-off process, the nanorods are denser.

2.2. Scanning Photoemission Microscopy

The growth behavior on N-face GaN substrate was further investigated by using scanning photoemission microscopy (SPEM), which presents spatially resolved elemental and chemical mapping with sub-micrometer resolution. **Figures 2**a and 2b show the SEM images of ZnO nanorods grown on n-GaN with the N-face exposed by a LLO process without the treatment. We intentionally performed the back-side lapping of the sapphire substrate to form the surface roughness. The incident

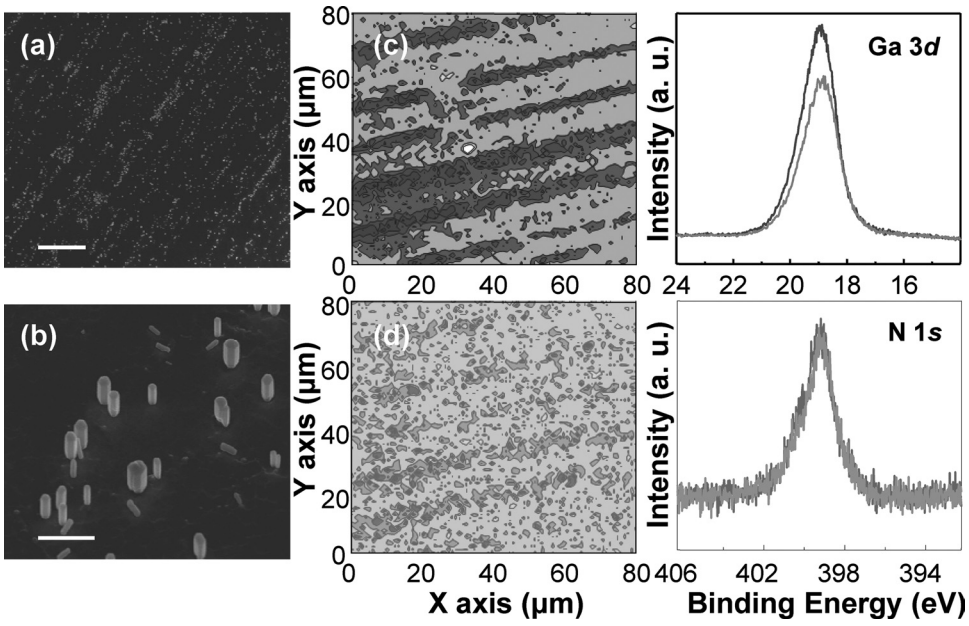

Figure 2. SEM images (a,b) of ZnO nanostructures grown on the epitaxial GaN with the n-face exposed by a laser lift-off process. The scale bar is 20 and 2 μm, respectively. Ga 3*d* (c) and N 1*s* (d) SPEM images, and Ga 3*d* and N 1*s* core level spectra for the sample prior to the UV/Ozone treatment. The result shows that the growth of ZnO nanorods may closely be related with the Ga concentration (or N-deficient region) at the surface.

laser could be scattered on the roughened surface during the LLO process, leading to the non-uniform distribution of laser intensity. As a result, it can be easily seen that the nanorods were aligned on the selective position without any additional process. For the origin of the selective growth, we investigated the surface chemistry of the n-GaN prior to the growth of nanorods. Figures 2c and d show Ga 3*d* and N 1*s* SPEM images, and Ga 3*d* and N 1*s* core level spectra. The SPEM image of Ga 3d can identify distinct regions showing deep blue, corresponding to the region on which nanorods are grown. From the Ga 3*d* core spectrum, we confirmed that the Ga concentration in the region showing a deep blue color was higher than that showing light blue. The higher Ga concentration does not indicate the formation of Ga-terminated surface. However, it is obvious that the growth was enhanced by the higher Ga concentration. In contrast, there is little change in the N concentration in N 1*s* SPEM results. We were also interested in whether or not there is any effect of oxygen and carbon concentration on the growth. Similarly, there is no change in O 1*s* and C 1*s* core level spectra (see Figure 2S in the Supporting Information). This shows that the growth of ZnO nanorods may closely be related with the Ga concentration (or N-deficient region) at the surface.

2.3. The Structural Properties of Grown ZnO Nanorods and ZnO/GaN Interface

The crystal structures of the ZnO nanorods grown on N-face GaN after UV radiation and ozone treatment were characterized by low-resolution and high-resolution TEM (HR-TEM) images, as shown in **Figure 3**. As shown in SEM images, it can be clearly seen that the nanorods grew vertically to about 200 nm in diameter and 1.5 μm in length (Figure 3a). The HR-TEM image and the corresponding diffraction pattern of the nanorods reveal highly ordered lattices, demonstrating that the nanorods are largely defect-free single crystals (Figure 3b). In addition, a selective area electron diffraction pattern taken along the $[1\bar{1}0]$ zone axis, together with measured lattice spacing of the adjacent planes, confirms that c-axial ZnO nanorods have $\{11\bar{2}0\}$ side planes, thus, non-polar planes comprise the side faces of the entire nanostructures. Furthermore, high magnification at the interface region where the tip joins to the substrate clearly shows the crystalline continuity between the substrate and the tip. Indeed, only very few (<4 nm) atomic layers are not well defined, as seen in Figures 3c and 3d. The structural evolution along the growth direction was reflected in FFT patterns. The GaN and ZnO diffraction patterns are seen as clear spots and the patterns in ZnO follow exactly the patterns in GaN, meaning that this may prove that ZnO nanorods with highly-crystalline properties grew epitaxially on GaN substrates. However, at the interface region, the diffraction spots were split into several smaller spots or became larger, suggesting the material crystallinity is degraded at the interfacial region.

In general, the strain between heteroepitaxial layers induces the formation of defects such as misfit dislocations and stacking faults to release the strain. Here, we mention the presence of stacking faults at the interfacial region, shown by the Fourier filtering image toward the [0002] direction (Figure 3e). The presence of such defects may explain effectively the defect (dislocation)-driven ZnO nanorod growth due to the inherent nature of GaN.[25] However, it is much worthier to mention that many ZnO nanorods can be successfully grown irrespective of the surface polarity. These defects are rarely observed in pure

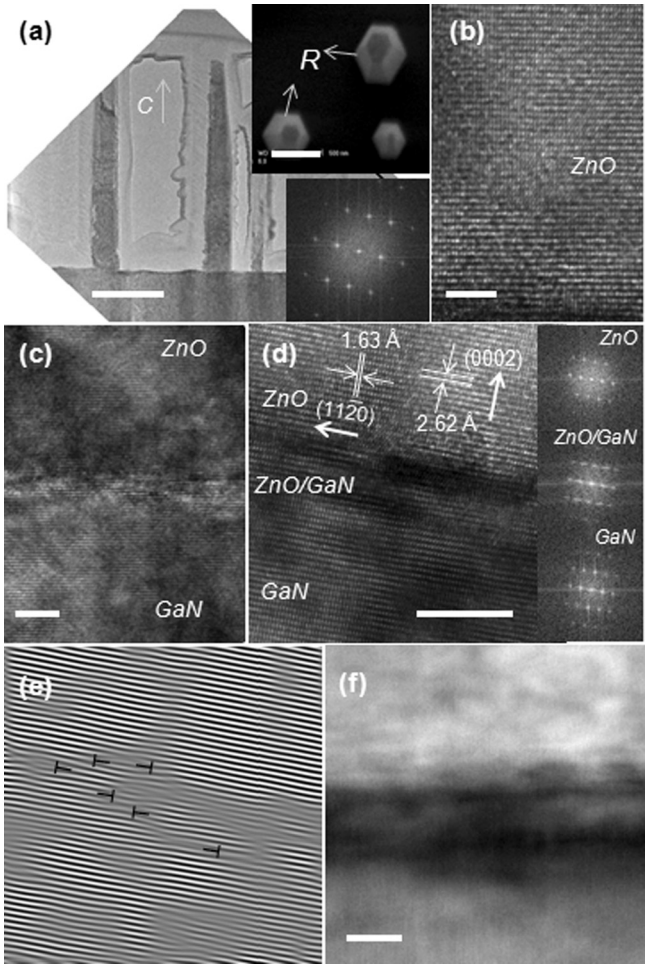

Figure 3. Transmission electron microscopy (TEM) images of ZnO nanorods grown on N-face n-GaN film. a) Low-magnification (the scale bar is 500 nm) and b) high-resolution TEM (HR-TEM) images (the scale bar is 2 nm) with its corresponding SAED pattern. c,d) HR-TEM images (the scale bar is 5 nm). e) Fourier-filtered image. f) HAADF-STEM image of the interstitial region between GaN and ZnO. c,d,e) The images show that lattice fringes of the nanorod and the substrate are parallel and continuous as if they were sculpted from a single crystal except the presence of a few stacking faults (the scale bar is 2 nm). The transition layer is less 4 nm thick.

ZnO nanorods, but the occurrence is increased at the interface (~4 nm), probably due to the lattice mismatch (~1.8%) between both structures. High-angle annular dark field (HAADF) scanning transmission electron microscopy (STEM) imaging, in which the contrast is directly related to the atomic number, shows that the change in atomic composition is clearly found at the interfacial region, thus, elemental analysis was done to investigate what happened at the this point.

Figure 4 shows an elemental map, determined by energy-dispersive X-ray spectroscopy (EDX), along a line traversing the interface between GaN and ZnO. The relative Ga and N concentrations, as a function of position, are shown in Figure 4b. It is immediately clear that Ga and Zn overlap in the interface region, and the Ga/N atomic ratio drastically decreases at this point, meaning that the surface region becomes rich in Ga with

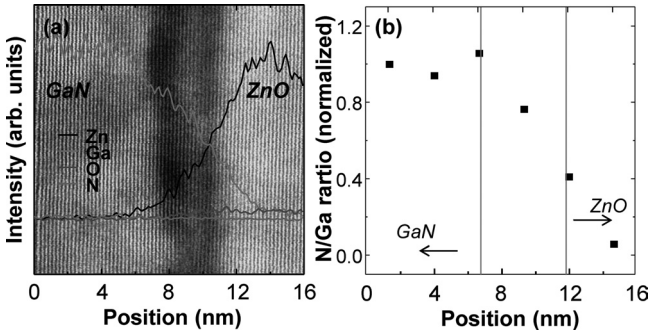

Figure 4. a) Elemental map, determined by EDX, along a line traversing the interface between GaN and ZnO. b) The relative Ga and N concentrations as a function of position shows that the growth can be enhanced by the structure control at the nanolevel of the surface.

this treatment. In the region where nanorods were not grown, the Ga/N ratio does not significantly decrease (see Figure 3S in the Supporting Information). This relative decrease in N atomic concentration at the interface region can be investigated with the valence band spectrum in Figure 5S. It is clearly seen that EF at the N (Ga) face substrate moved by 0.46 eV (0.37 eV) toward EC because of the treatment, meaning the formation of the N-deficient region. We annealed the n-face GaN at 900 °C under a vacuum (<100 mTorr) in order to investigate the effects of N-deficiency on the ZnO nanorods' growth. Such a high temperature annealing is well-known as an effective method to produce high numbers of nitrogen vacancies due to the out-diffusion of nitrogen atoms. As a result, SEM images (Figure 4S) showed that the nanowires growth was enhanced by the annealing process.

The observed interdiffusion of Zn and O into GaN epitaxial layers, and Ga and N into ZnO substrate have been commonly observed when the layers were deposited at high temperature (>800 °C).[26,27] The interfacial cubic layer (Ga_2O_3 or Zn_3N_2), known to have inversion symmetry in GaN/ZnO materials, was possibly ascribed to the interfacial interdiffusion. However, the growth temperature is not very high (~90 °C) and it is unlikely that Zn atoms easily diffuse into GaN substrates at such a low temperature. Such secondary phases were also not produced at the interface. No Zn atoms were detected on the surface of bare N-face GaN, resulting in growing very few or negligible nanorods, which may prove this definitely. By contrast, by a statistical characterization of the diffusion, it can be expected that the Zn or O adatoms can move by a defect-mediated mechanism (the vacancy-mediated diffusion) into the GaN substrates, and act as seeds for the nanorods' growth. Furthermore, the dissociation of the surface chemical group will change the surface stoichiometry (i.e., Ga rich), generating the surface charges, which will result in dramatic increases in nucleation sites for nanorod growth.

2.4. Properties of ZnO Nanorods/Vertical Structured InGaN LEDs

This approach was used to evaluate the light output characteristics of vertical LEDs. **Figure 5** shows optical microscope images

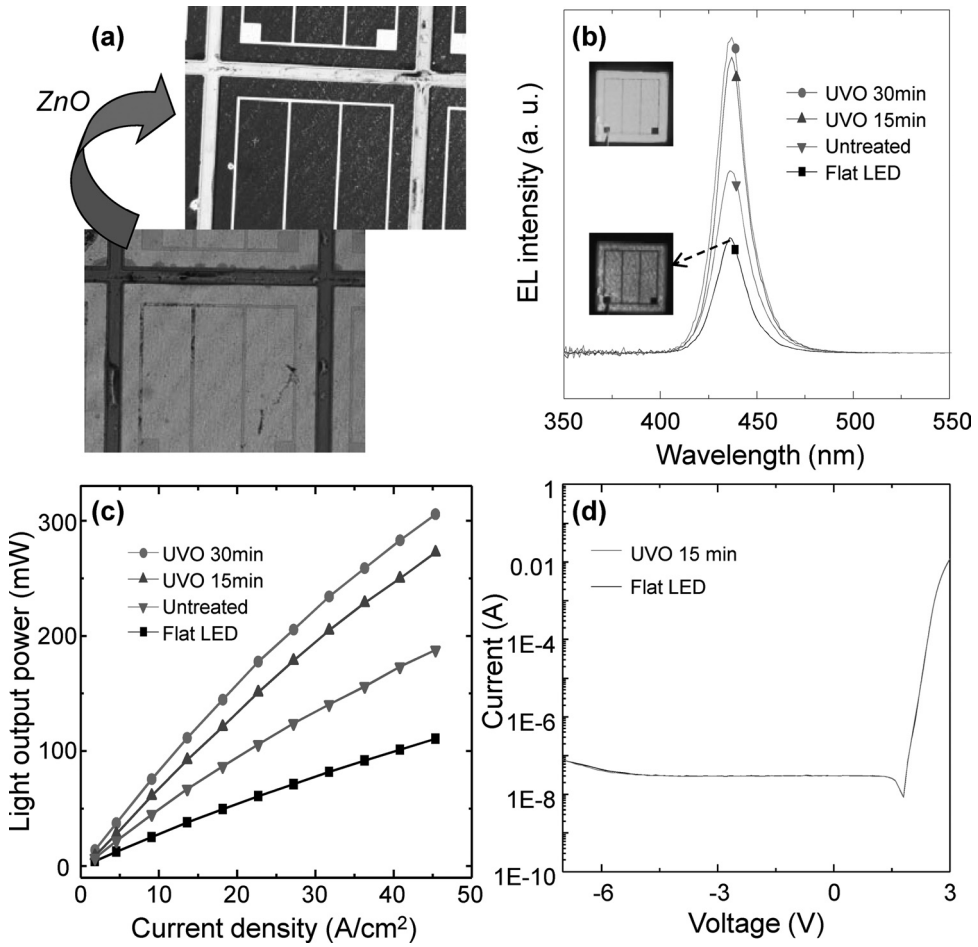

Figure 5. a) Optical microscopy images of vertical-structured LEDs before and after ZnO nanorods growth. b) EL spectra measured at 45 A cm^{-2} and c) light output power vs. injection current density (*L–I*) of VLEDs for ZnO nanorods, compared with flat VLED. *I–V* characteristics are also shown in (d) after UV/Ozone treatment.

of V-LEDs before and after ZnO nanorods' growth, showing that the nanorods are distributed quite uniformly. Employing the ZnO nanorods on N-face GaN surface increases the light extraction of the LED by about 69%, showing a similar level of light extraction enhancement, as reported in the literature (Figure 5b). However, dramatic increase (~2.5 times) in the light extraction efficiency and output power of the vertical LEDs was achieved by the UV radiation and Ozone treatment prior to the growth. As the treatment time increases to 30 min, the light emission and output power increased by about 2.81 times, measured at 45 A cm^{-2}. The current–voltage (*I–V*) characteristics of vertical structured LEDs were also shown. The forward voltages of vertical LEDs with flat n-GaN and ZnO/GaN layers at an injection current of 20 mA are 2.8 V and 2.81 V, respectively. Furthermore, the reverse leakage currents of vertical LEDs remained unchanged after the growth of nanorods. These results show that the formation of ZnO nanorods does not cause the deterioration of electrical properties.

The 3D finite-difference time-domain (FDTD)-based simulation was done for numerical analysis of the light output power and far-field emission pattern for V-LEDs with ZnO nanorods, as shown in **Figure 6**. Figure 6a shows that the simplified V-LED structures for FDTD simulation consists of a 2-μm thick n-GaN layer, a 100-nm thick InGaN/GaN MQW active layer, a 200-nm thick p-GaN layer, and 300-nm thick Ag reflectors. A point source that is put in the middle of the MQW layer is regarded as the light source. For the conventional flat V-LEDs, the far-field pattern shows perfect circular symmetry due to the total internal reflection at GaN/air interface. The light escape angle is very small (less than 40°) and only a small part of the surface has emission light. The inner and outer radiation ring was ascribed to the direct emission from the InGaN MQW and the reflected emission by the Ag reflector, respectively. When ZnO nanorods were employed on the surface, the irregular and scattered radiation pattern was shown, and the light intensity distribution map spread over the entire surface, meaning that the light escape angle was significantly enlarged to over 75°. The enhancement of light output power in V-LEDs with ZnO nanorods was about 3.01 times, well in agreement with experimental results as shown in Figures 5b and 5c. This enhancement of light output power in V-LEDs with ZnO nanorods could be explained by elimination of guided modes in ZnO nanorods.

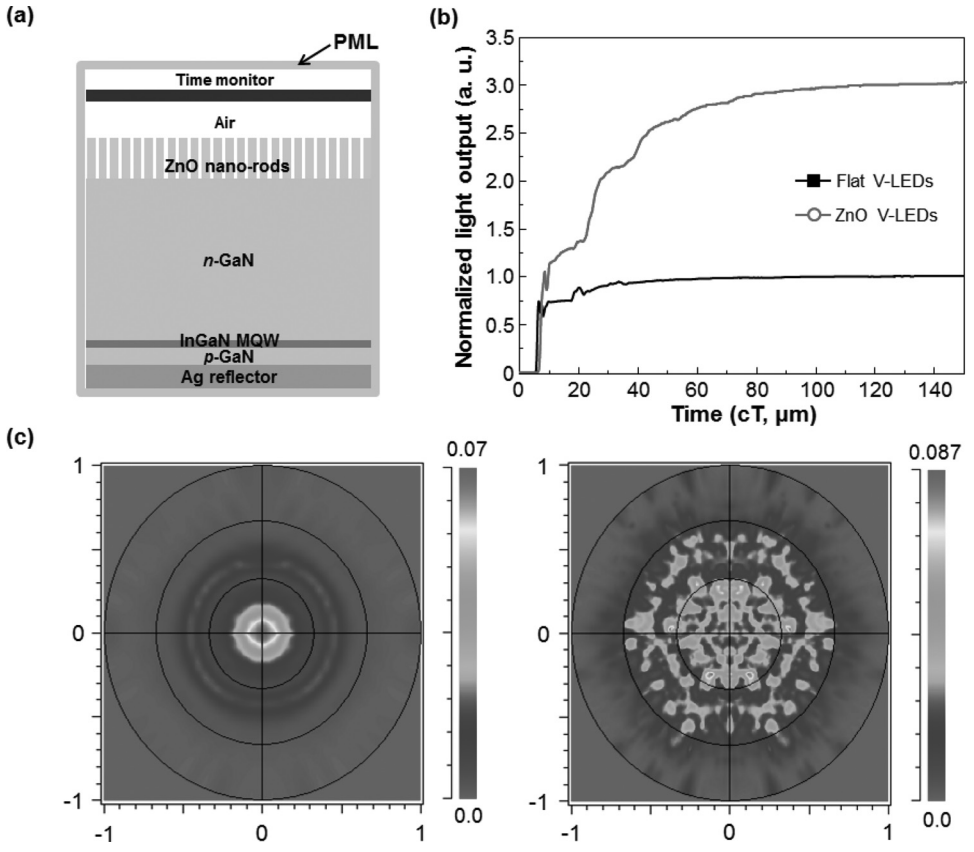

Figure 6. a) Schematic side-view structure of the V-LEDs with ZnO nanorods for numerical analysis. b) Normalized light output power as a function of simulation time for the V-LEDs with flat n-GaN surface and ZnO nanorods structures. c) Simulated polar projection of far-field intensity for the flat n-GaN (left) and ZnO nanorods (right) V-LEDs.

The normalized light output power of V-LEDs was increased with ZnO nanorod's diameter as shown in Figure 6*S*a, because the more light with wavelength of 450 nm could be put into the ZnO nanorods with larger diameter. However, the increase ratio of light output power was smaller than that of area fraction of ZnO nanorods, and this could be due to the increased number of guided modes in ZnO nanorods with larger diameter (see Figure 6Sb in the Supporting Information), resulting in the reduction of light extraction from ZnO nanorods.[28]

According to the above view, the extreme enhancement in light extraction (2.81×) will be ascribed to the successful growth of highly-dense nanorods on the N-face n-GaN, as explained by the wave-guiding effect, due to the refractive index difference between ZnO (n = 2.1) and air (n = 1).[25] When the photons generated in the active region escape the surface, the light extraction efficiency will be mainly influenced by two factors (except the refractive index). Assuming that the interaction between the ZnO and GaN layers is significant, the stacking faults or strain, which may absorb light passing through the interface, were induced at the interface. However, the losses in the light emission at the interface were considered negligible and not included in the simulation. Thus, the strong agreement between the simulation predictions and experimental results indicates that ZnO nanorods are well-grown epitaxially on the GaN layer. Second, it is clearly seen that there is still room for the nanorods, as they occupy only about 60% of the entire surface.

Figure 7S in the Supporting Information shows the light output with the degree of occupancy (%) obtained from the experimental results, showing the significant increase of light extraction efficiency at ~50%. Interestingly, the light extraction efficiency was further increased by about 30% by depositing 1-μm-thick MgO layer on ZnO nanorods by e-beam evaporation, compared with V-LEDs with only ZnO nanorods. Also of note is the improvement in the uniformity of the diameter, which may increase the light extraction efficiency. Thus, the light extraction efficiency can be further improved by optimized design and intensive analysis of nanogeometry, expecting larger enhancement than that (~3×) of PCE-assisted V-LEDs.

3. Conclusions

In summary, we demonstrated the successful growth of -densly aligned ZnO nanorods with great vertical alignment on N-face n-GaN, followed by the fabrication of vertical LEDs with a GaN/ZnO hybrid structure showing an extreme enhancement in the light extraction efficiency (~3.0×). The structural transformation (i.e., dissociation of the surface nitrogen atoms) at the nanolevel by the UV radiation and Ozone treatment contributed

significantly to the initial nucleation for nanorod growth due to interdiffusion of Zn into GaN, evident by the SPEM, HRTEM, and ultraviolet photoelectron spectroscopy (UPS) measurements. This enabled the growth of densely aligned ZnO nanowires with great vertical alignment epitaxially on N-face n-GaN. This approach was applied to fabricate the vertical LEDs, showing an extreme enhancement in light extraction efficiency (>2.8×) compared with flat V-LEDs, and strong agreement with the simulation expectations (~3.01×) obtained from FDTD tools by wave-guiding effect. The further increase (~30%) in light extraction efficiency is observed by optimized design and intensive analysis of nanogeometry (MgO layer on ZnO nanorods). This rational engineering of substrates by a structural transformation at the nanolevel may provide a promising method for producing highly dense one-dimensional nanomaterials for applications of optoelectronic devices.

4. Experimental Section

LED Fabrication: A 500-nm-thick undoped GaN buffer layer, a 4-μm-thick n-type GaN, an InGaN/GaN MQW active region, a p-type AlGaN electron blocking layer, and a p-type GaN layer were grown in sequence on c-plane sapphire substrates using metal-organic chemical vapor deposition. V-LEDs (1 mm × 1 mm) were fabricated on the substrate. Active regions were defined by dry etching into the sapphire substrate. Ag-based contacts were deposited on p-GaN and this was followed by annealing at 450 °C for 2 min in ambient air. A 50 mm thick Ni layer was electroplated on the p-contacts as a platform and subsequently the LLO process for separating the MQW LED/Ni structure from the sapphire substrate was performed in air using a Lambda Physik Lextra 200 KrF pulsed excimer laser. After the LLO, Cr/Au n-contacts were deposited on n-GaN, forming n-side-up vertical InGaN LEDs on the silicon wafer.

Growth of ZnO Nanorods: ZnO nanorod arrays were then grown on the n-GaN surface of the V-LEDs. Before the growth, the substrates were transferred to an exposure chamber specified for UV/Ozone treatment, and exposed for 15 and 30 min to investigate the effects of the exposure time on the growth. According to our previous results, the UV radiation and ozone treatment allow for formation of heterogeneous surface structures at the nanolevel as well as the modification of surface stoichiometry, generating surface charge, and acting as nucleation sites for the nanorods' growth. This observation shows the possibility that the method will be useful for the nanorods' growth on N-face GaN. The substrates were then put face down, floating on the nutrient growth solution (1: 1 ratio of zinc nitrate and hexamethylenetetramine (HMTA) 2 mM) and were kept in an oven at 90 °C for 3 h. After that, the V-LEDs were removed from the aqueous solutions, and rinsed with distilled water.

Characterization: The light output power of V-LEDs was measured with an unpacked (on-wafer) configuration using an integrating sphere. To investigate the surface chemistry of the n-GaN layer, scanning photoemission microscopy (SPEM) was used at the 8A1 undulator beamline in the Pohang Accelerator Laboratory (PAL). SPEM is a powerful tool for investigating the chemical information of the local surface area. By combining spatially resolved elemental and chemical mapping with sub-micrometer resolution photoemission spectroscopy, SPEM can provide quantitative and qualitative information with high lateral and energy resolution. The lateral space resolution was less about 1 μm. A hemispherical electron energy analyzer with 16 energy-detecting channels/windows was used, and the energy separation/resolution per window was 0.8 eV. UPS was also employed to study valence energy levels and chemical bonding. SPEM was done using a PHILIPS XL30S with an accelerating voltage of 5 kV. The high-resolution transmission electron microscopy (HR-TEM) images were collected using a Cs-corrected JEM-2100 operated at 200 kV.

The three-dimensional (3D) finite-difference time-domain (FDTD) method with a perfectly matched layer (PML) was also employed for numerical analysis of the light output power, consistent with the extreme enhancement in the light extraction efficiency of about 2.81 times. The geometry of the ZnO nanorods was described as 50-periods hexagonal arrays with diameter, length and pitch of 200, 500, and 300 nm, respectively. The diameter and pitch were determined by high-magnification scanning electron microscopy (SEM) images. A point dipole polarized along the *x*, *y*, and *z* direction was used as a radiating source. The wavelength of the light source was set to 450 nm. Furthermore, the diameter of ZnO nanorods was changed from 200 to 500 nm to explain the effect of ZnO nanorods diameter on light extraction efficiency of V-LEDs with ZnO nanorods. The gap between ZnO nanorods was fixed at 100 nm.

Supporting Information

Supporting Information is available from the Wiley Online Library or from the author.

Acknowledgements

This research was supported by the National Research Foundation of Korea (NRF) grant funded by the Korea government (MEST) (No. 2011-0004465) and by the Industrial Technology Development Program funded by the Ministry of Knowledge Economy (MKE, Korea). We are very thankful to Professor Martin Moskovits (UCSB) and Professor Zhong Lin Wang (Georgia Tech.) for fruitful discussions.

Received: August 23, 2011
Revised: October 26, 2011
Published online: December 8, 2011

[1] S. Pimputkar, J. S. Speck, S. P. DenBaars, S. Nakamura, *Nat. Photonics* **2009**, *3*, 180.
[2] S. Noda, M. Fujita, *Nat. Photonics* **2009**, *3*, 129.
[3] H. W. Jang, S. W. Ryu, H. K. Yu, S. H. Lee, J.-L. Lee, *Nanotechnology* **2010**, *21*, 025203.
[4] S. J. Wang, K. M. Uang, S. L. Chen, Y. C. Yang, S. C. Chang, T. M. Chen, C. H. Chen, B. W. Liou, *Appl. Phys. Lett.* **2005**, *87*, 011111.
[5] D. Fuhrmann, C. Netzel, U. Rossow, A. Hangleiter, G. Ade, P. Hinze, *Appl. Phys. Lett.* **2006**, *88*, 071105.
[6] E. F. Schubert, *Light Emitting Diodes*, 2nd Ed., Cambridge University Press, Cambridge, UK **2006**.
[7] T. Fujii, Gao, Y. R. Sharma, E. L. Hu, S. P. DenBaars, S. Nakamura, *Appl. Phys. Lett.* **2004**, *84*, 855.
[8] M. Megens, A. David, J. J. Wierer, *Nat. Photonics* **2009**, *3*, 163.
[9] J. K. Kim, S. Chhajed, M. F. Schubert, E. F. Schubert, A. J. Fischer, M. H. Crawford, J. Cho, H. Kim, C. Sone, *Adv. Mater.* **2008**, *20*, 801.
[10] H. Jia, L. Guo, W. Wang, H. Chen, *Adv. Mater.* **2009**, *21*, 4641.
[11] H. M. Kim, D. S. Kim, Y. S. Park, D. Y. Kim, T. W. Kang, K. S. Chung, *Adv. Mater.* **2002**, *14*, 991.
[12] A. C. Tamboli, K. C. McGroddy, E. L. Hu, *Phys. Status Solidi C* **2009**, *6*, S807.
[13] J. Zhong, H. Chen, G. Saraf, Y. Lu, C. K. Choi, J. J. Song, D. M. Mackie, H. Shen, *Appl. Phys. Lett.* **2007**, *90*, 203515.
[14] K.-K. Kim, S.-D. Lee, H. Kim, J.-C. Park, S.-N. Lee, Y. Park, S.-J. Park, S.-W. Kim, *Appl. Phys. Lett.* **2009**, *94*, 071118.
[15] C. H. Chao, W. H. Lin, W. H. Chen, C. H. Changjean, C. F. Lin, *Semicond. Sci. Technol.* **2009**, *24*, 105017.

[16] K. S. Kim, S.-M. Kim, H. Jeong, M. S. Jeong, G. Y. Jung, *Adv. Funct. Mater.* **2010**, *20*, 1076–1082.
[17] K. Dai, C. B. Soh, S. J. Chua, L. Wang, D. Huang, *J. Appl. Phys.* **2011**, *109*, 083110.
[18] Z. L. Wang, X. Y. Kong, J. M. Zuo, *Phys. Rev. Lett.* **2003**, *91*, 185502.
[19] T. Song, J. W. Choung, J.-G. Park, W. I. Park, J. A. Rogers, U. Paik, *Adv. Mater.* **2008**, *20*, 4464.
[20] C. H. Chiu, C. E. Lee, C. L. Chao, B. S. Cheng, H. W. Huang, H. C. Kuo, T. C. Lu, S. C. Wang, W. L. Kuo, C. S. Hsiao, S. Y. Chen, *Electrochem. Solid-State Lett.* **2008**, *11*, H84.
[21] Q. Li, V. Kumar, Y. Li, H. Zhang, T. J. Marks, R. P. H. Chang, *Chem. Mater.* **2005**, *17*, 1001.
[22] J. L. Rouviere, J. L. Weyher, M. Seelmann-Eggebert, S. Porowski, *Appl. Phys. Lett.* **1998**, *73*, 668.
[23] M. Aoki, H. Yamane, M. Shimada, T. Kajiwara, S. Sarayama, F. J. Disalvo, *Cryst. Growth Des.* **2002**, *2*, 55.
[24] B.-U. Ye, H. K. Yu, M. H. Kim, J.-L. Lee, J. M. Baik, *J. Phys. Chem. C* **2011**, *115*, 7987.
[25] S. A. Morin, S. Jin, *Nano Lett.* **2010**, *10*, 3459.
[26] T. Suzuki, C. Harada, H. Goto, T. Minegishi, A. Setiawan, H. J. Ko, M.-W. Cho, T. Curr Yao, *Appl. Phys.* **2004**, *4*, 643.
[27] S. K. Hong, T. Hanada, H. J. Ko, Y. Chen, T. Yao, D. Imai, K. Araki, M. Shinohara, K. Saitoh, M. Terauchi, *Phys. Rev. B* **2002**, *65*, 115331.
[28] M.-L. Kuo, Y.-S. Kim, M.-L. Hsieh, S.-Y. Lin, *Nano Lett.* **2011**, *11*, 475.